Journal of Electromyography and Kinesiology 48 (2019) 1–8

Contents lists available at ScienceDirect

Journal of Electromyography and Kinesiology

journal homepage: www.elsevier.com/locate/jelekin

Influence of experimental pain on the spatio-temporal activity of upper trapezius during dynamic lifting – An investigation using Bayesian spatio-temporal ANOVA

Bernard X.W. Liew[a,*], Yu (Ryan) Yue[b], Corrado Cescon[c], Marco Barbero[c], Deborah Falla[a]

[a] Centre of Precision Rehabilitation for Spinal Pain (CPR Spine), School of Sport, Exercise and Rehabilitation Sciences, College of Life and Environmental Sciences, University of Birmingham, Birmingham, United Kingdom
[b] Paul H. Chook Department of Information Systems and Statistics, Zicklin School of Business, Baruch College, The City University of New York, United States
[c] Rehabilitation Research Laboratory 2rLab, Department of Business Economics, Health and Social Care, University of Applied Sciences and Arts of Southern Switzerland, Manno, Switzerland

ARTICLE INFO

Keywords:
Pain
Electromyography
Motor control
Spatio-temporal
Bayesian

ABSTRACT

High-density surface electromyography (HDsEMG) provides a detailed analysis of a muscle's spatial distribution of activity. We applied a Bayesian spatio-temporal statistical method to quantify how acute nociception and task repetition alters the upper trapezius instantaneous spatial distribution of activity during dynamic muscular contractions. Ten male adults performed repeated lifting of a 1 kg box between shelves positioned at hip and shoulder heights with a cycle time of 3 s for 50 cycles under four conditions: baseline, isotonic and hypertonic saline injections (nociception) to the right upper trapezius, and 15 min post injection. Activity of the right upper trapezius was measured using a 64-channel surface electrode grid. Statistical inference was performed using Integrated Nested Laplace Approximations (INLA), and significance was determined by a non-zero crossing of the Bayesian 95% credible intervals (CrI). The maximal decrease in activity after nociception was −38.1 μV [95% CrI −40.9 to −35.3] at 30% of the lift cycle when compared to baseline. The maximal reduction in muscle activity between the early and later phases of lifting in the presence of nociception was by 10.4 μV [95% CrI 8.2–12.6]. A more holistic understanding of muscle behaviour is achieved using spatio-temporal inference than traditional reductionist methods.

1. Introduction

High-density surface electromyography (HDsEMG) has been increasingly used to study how pain (Falla et al., 2017), fatigue (Abboud et al., 2016), and repetitive task execution (Samani et al., 2017) alter the spatial distribution of EMG amplitude. Changes in the spatial distribution of EMG amplitude reflect a variety of physiological (mal) adaptations. For example, the spatial distribution of intra-muscular activity may reflect the intrinsic variation of motor neuron activity for load distribution (Martinez Valdes et al., 2018); a non-uniform distribution of nociceptive input to motor neurons (Dideriksen et al., 2016); and a strategy to sustain consistent force outputs (Falla and Farina, 2008a). Intra-muscular coordination of the upper trapezius has been widely investigated, since this muscle is commonly implicated in the development of musculoskeletal pain and fatigue syndromes (Falla et al., 2017; Samani et al., 2017).

Excitation of nociceptors within the upper trapezius muscle via injection of hypertonic saline, has been shown to shift the barycentre of muscle activity caudally (Falla et al., 2009; Falla et al., 2017; Madeleine et al., 2006, Dideriksen et al., 2016). Whether motor adaptations to a noxious stimulus is specific to the site of nociception remains unclear (Falla et al., 2009; Gallina et al., 2018; Hug et al., 2013). For instance, a caudal shift in barycentre of upper trapezius activity occurred regardless of the site of nociception within the muscle (Falla et al., 2009; Dideriksen et al., 2016). At the vastus medialis, the region with the greatest reduction in EMG amplitude was at the site of nociception (Gallina et al., 2018); whereas Hug et al. (2013) reported that the reduction in discharge rate of soleus motor units was greatest in the region of nociception, but this was not observed in all participants. It is evident from the topographical EMG amplitude maps of the two studies (Falla et al., 2009, Gallina et al., 2018), that different sites of nociception could change the spatial distribution of muscle activity differently. For example, a cranial injection to the upper trapezius appear to reduce cranial muscle activity only, whilst a caudal injection to the

* Corresponding author.
E-mail address: LiewB@adf.bham.ac.uk (B.X.W. Liew).

https://doi.org/10.1016/j.jelekin.2019.05.018
Received 24 January 2019; Received in revised form 21 May 2019; Accepted 30 May 2019

same muscle appear to reduce muscle activity (albeit non-symmetrically) in both the cranial and caudal muscle regions (Falla et al., 2009).

Inconsistency in defining the nature of motor adaptations relative to the site of noxious stimulation could be due to a myriad number of plausible surface EMG spatial distribution patterns bringing about similar shifts in the barycentre. The sensitivity of inferring a complex spatial EMG distribution from its barycentre may also depend on the physical dimension and number of channels within the electrode grid. To understand the spatial distribution of EMG amplitude driving a change in the position of the barycentre, researchers have qualitatively drawn on observations from topographical EMG amplitude maps.

It is also unclear if the effect of nociception on the spatial distribution within the upper trapezius remains consistent during a repetitive dynamic task. Experimental pain induced a caudal shift in the barycentre of the upper trapezius during an isometric contraction, and this caudal shift persisted for the entire duration of the contraction (60–90 s) (Falla et al., 2009, Madeleine et al., 2006). Although Falla et al. (2017) collected EMG data over 50 lifting repetitions, the authors did not investigate whether adaptations of the upper trapezius during nociceptor excitation changed across repetitions of this dynamic motor task. However, there is evidence from a pain-free cohort that repetitive dynamic movements resulted in a significant lateral shift of the upper trapezius's barycentre of activity (Samani et al., 2017). Knowing if motor adaptations to nociception is magnified or reduced by repeated performance is fundamental towards understanding the mechanisms related to the development of work-related neck-shoulder disorders.

HDsEMG data has a spatial component due to the two-dimensional coordinate system of the electrode grid. Since muscle activity is assessed across time, there is also a temporal component (Falla et al., 2017, Madeleine et al., 2006). Spatio-temporal HDsEMG has always been summarized into discrete metrics, such as the barycentre. In the present study, a discrete variable is one which has only magnitude and no space/time information. Although analysing spatio-temporal data in a discrete form does not provide a comprehensive understanding of physiological mechanisms, an advantage is that it allows for simpler statistical inference methods (e.g. Analysis of Variance [ANOVA]). However, performing statistical inference on discrete HDsEMG data is not without problems. As the number of repeated tests increases, either the inflation of the familywise Type I error rate gets severely inflated when no efforts are made to control the familywise error rate, or the statistical power diminishes when an attempt is made to control the familywise error rate.

In the present study, Bayesian spatio-temporal ANOVA (Wang et al., 2018, Yu et al., 2018) was used to perform a secondary analysis on previously published data investigating the influence of experimentally induced upper trapezius muscle pain on spatio-temporal activity of the upper trapezius during a repeated lifting task (Falla et al., 2017). The aim of the present study was to quantify the spatial distribution of upper trapezius activity that accounts for the reported shifts in its barycentre of activity under nociception (Falla et al., 2017). Three hypotheses are proposed: First, hypertonic saline injection to the cranial portion of the upper trapezius would only reduce muscle activity in the cranial region of the muscle (Falla et al., 2009). Second, the reduction in cranial muscle activity after hypertonic saline injection would be symmetrical in the medial-lateral direction (Falla et al., 2017). Third, hypertonic saline injection would reduce the activity of the lateral portion of the upper trapezius more during the early than later phase of lifting (Samani et al., 2017) - findings not observed in the original study (Falla et al., 2017).

2. Methods

2.1. Design, participants, task

This was a secondary analysis of a previously published study, where full details of the experimental procedures have been previously reported (Falla et al., 2017). The study was approved by the local Ethics Committee (#200538), conducted according to the Declaration of Helsinki and all participants provided written informed consent prior to their study inclusion. Ten healthy male volunteers with a mean (standard deviation [sd]) age, height and weight of 26.2 (3.1) years old, 1.78 (0.06) m, and 71.3 (9.2) kg, respectively, participated and all participants completed the study.

Participants attended a single laboratory session and were required to lift a 1 kg box between shelves positioned at hip and shoulder height, with a cycle time of 3 s for 50 cycles. An acoustic signal from a digital metronome was provided to the subjects during the task to standardize the duration of cycles. Subjects repeated the task four times: (1) baseline no injection, (2) isotonic saline (0.9%) injection to the cranial portion of right upper trapezius, (3) hypertonic saline (5.8%) injection to the same portion of the upper trapezius, and (4) recovery (15 min post hypertonic injection). The order of conditions was not randomized. The rest interval between the repetitions was set to 15 min starting from the moment when the pain caused by the injections disappeared. Subjects practiced the movement sequence for ~1 min without the weight prior to data recording.

The experimental muscle pain was induced by injection (27G cannula) of 0.4 ml sterile hypertonic saline (5.8%) into the upper division of the trapezius on the right side with the subject seated. Isotonic saline (0.4 ml, 0.9%) was used as a control injection in a similar location. The location of the injection was defined as 15 mm cranial to the line between the acromion and the spinous process of the seventh cervical vertebra. The bolus was injected over a 10-s period. The isotonic saline injection was given first however participants were blinded to each injection and were told that one or both might be painful.

2.2. HDsEMG

HDsEMG signals were recorded from the right upper trapezius using a 64-electrode adhesive electrode grid (ELSCH64NM3, OT Bioelettronica, Torino, Italy) (Fig. 1). The 64 electrodes were arranged in a 13 row by 5 column grid (1 mm diameter, 8 mm inter-electrode distance), with an absent electrode in the upper right corner. The electrode grid was placed with the fourth row along the line between the lateral edge of the acromion and C7, with the lateral column 10 mm distant from the innervation zone (Falla et al., 2017). The injections were performed lateral to the electrode grid (~10 mm) and corresponded to the 4th row of the grid.

EMG signals were amplified 2000 times and sampled at 2048 Hz (EMGUSB2, OT Bioelettronica, Torino, Italy). Four accelerometers were positioned on the box and the four signals were averaged to produce a single signal, which was subsequently rectified and filtered (low pass, 2nd order Butterworth at 10 Hz). A 50 m/s^2 threshold on the filtered accelerometer signal was used to identify the contact instants of the box with each of the 2 shelves, to obtain the beginning and end time points of a lifting repetition.

2.3. Signal processing

HDsEMG signals were filtered with a 2nd order Butterworth bandpass filter (10–400 Hz). Each lift cycle was discretized into ten 10% time epochs. Single differential channels were extracted from each pair of electrodes in the horizontal direction, resulting in a 13 × 4 grid of 51 bipolar channels, with one missing channel on the upper right corner. The single differential method was used to reduce the non-propagating components such as end of fibre effects, which is a common procedure in surface EMG processing. RMS values from each differential channel were calculated for each 10% epoch. This produced a 10 × 51 (time by channels) matrix of RMS values for each participant, condition, and each lifting repetition. Twelve participant-condition combinations had less than 50 repetitions of HDsEMG data, due to significant signal

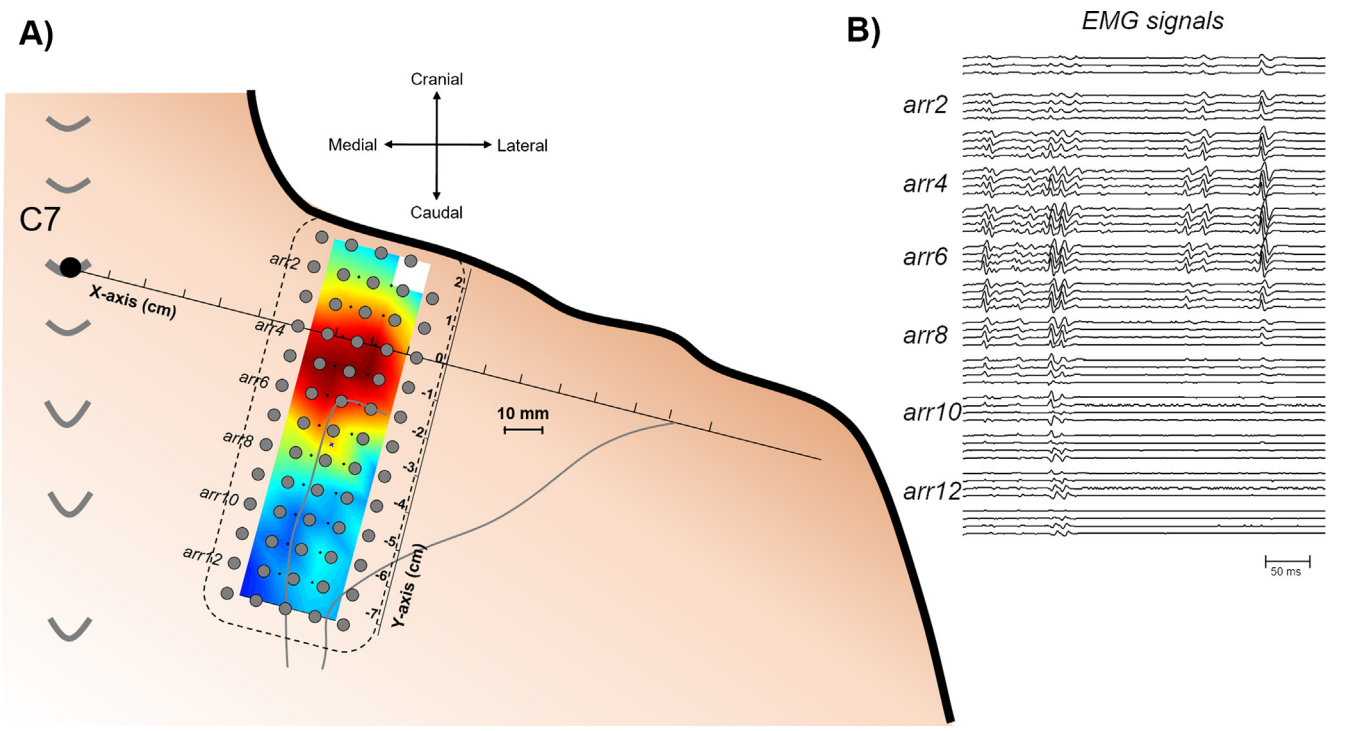

Fig 1. (A) High-density surface electromyography signals were detected using a 13 rows by 5 columns adhesive grid (1 mm diameter, 8 mm inter-electrode distance) of electrodes over the right upper trapezius muscle. Injection was performed 10 mm lateral to the electrode grid and 15 mm cranial to the line joining the acromion and the spinous process of the C7 vertebra. (B) Example of one subject raw EMG signals across the electrode grid.

artefacts present within the accelerometer signals, precluding the identification of a lifting repetition. The minimum number of lifting repetitions available was 39. Thirty-eight available repetitions were used from each participant and condition to allow pairwise difference in EMG signals to be computed (see below). Lifting repetitions were dichotomized into "early phase" (first 19 available repetitions) and "later phase" (second 19 available repetitions).

2.4. Outcome variables

There were six outcome variables, with the first three being:

$$\Delta EMG_{i=1,2,3}^{early} = EMG_{hypertonic} - EMG_{baseline,isotonic,recovery} \quad (1)$$

where $\Delta EMG_{i=1}^{early}$, $\Delta EMG_{i=2}^{early}$, $\Delta EMG_{i=3}^{early}$ represented the difference in the 10 × 51 matrix values of EMG RMS (μV) at each epoch between hypertonic saline injection vs baseline, hypertonic vs isotonic injections, and hypertonic injection vs recovery during the early lift phase, respectively. A negative $\Delta EMG_{i=1,2,3}^{early}$ indicated a reduction in EMG amplitude with the hypertonic saline injection, relative to its comparator. The other three outcomes were:

$$\Delta EMG_{phase}^{i=1,2,3} = \Delta EMG_{later}^{i=1,2,3} - \Delta EMG_{early}^{i=1,2,3} \quad (2)$$

where $\Delta EMG_{phase}^{i=1,2,3}$ represented the difference in the 10 × 51 matrix values of EMG RMS (μV) at each epoch between the later and early phase of lifting. If $\Delta EMG_{early}^{=1,2,3}$ is negative, than a positive $\Delta EMG_{phase}^{i=1,2,3}$ indicates a greater reduction in EMG amplitude in the early than later phase.

2.5. Statistical inference

A two-way mixed-effects spatio-temporal ANOVA model with a random subject-intercept of the form was fitted,

$$y_i = \eta(x_i) + b_{g_i} + e_i \quad \text{for } i = 1, \cdots, n \quad (3)$$

where n is the total number of data points for all participant-condition combinations after converting the data into a column vector, y_i is the ΔEMG in Eqs. (1) and (2), $x_i = (t_i, s_i)$ is the fixed effect of lifting cycle (t_i) and spatial location of the electrode grid (s_i), g_i is the subject indicator, b_{g_i} is the random effect such that $b_{g_i} \overset{iid}{} N(0, \delta)$ with $\delta > 0$, and $e_i \overset{iid}{} N(0, \sigma^2)$ is the random error. t_i represents the 10 epochs of the lifting cycle, whilst s_i represents the 51 bipolar channels. The predictor η can be further decomposed into main and interaction effects as follows:

$$\eta(x_i) = \eta_1(t_i) + \eta_2(s_i) + \eta_{12}(t_i, s_i) \quad (4)$$

where η_1 is the main temporal effect of lifting cycle, η_2 is the main spatial effect of electrode grid location, and η_{12} is the spatio-temporal interaction effect. We fitted model (3) under a fully Bayesian framework. For the η_1 main temporal effect, a first order autoregressive (AR1) prior was used (Wang et al., 2018). For the spatial effect η_2, a stochastic partial differential equation (SPDE) spatial prior was used. For the interaction effect η_{12}, a separable spatio-temporal prior was used (Cameletti et al., 2013).

The resulting Bayesian mixed model can be efficiently estimated using integrated nested Laplace approximations (INLA) (Wang et al., 2018). INLA provides accurate approximated posterior distributions of all parameters (e.g. β coefficients) given the data, needed to make fully Bayesian inference (i.e. posterior mean with credible intervals [CrI]). The technical details of INLA can be found in the supplementary material (Rue et al., 2009). For the main and interaction effects, we calculated the posterior joint probabilities for a change in any EMG channel across the electrode grid to produce a topographical map of probabilities (Bolin and Lindgren, 2015). The probability map provides useful visualization of the certainty of where and when any EMG amplitude changes occur. To quantify the magnitude of EMG changes on all spatial locations and across the lifting cycles, and to determine if these changes were significant, the mean and 95% CrI was calculated. Significant changes were defined within a Bayesian framework, by a non-zero crossing of the 95% CrI. We provide the data, code, and results in a public repository (Liew et al., 2018).

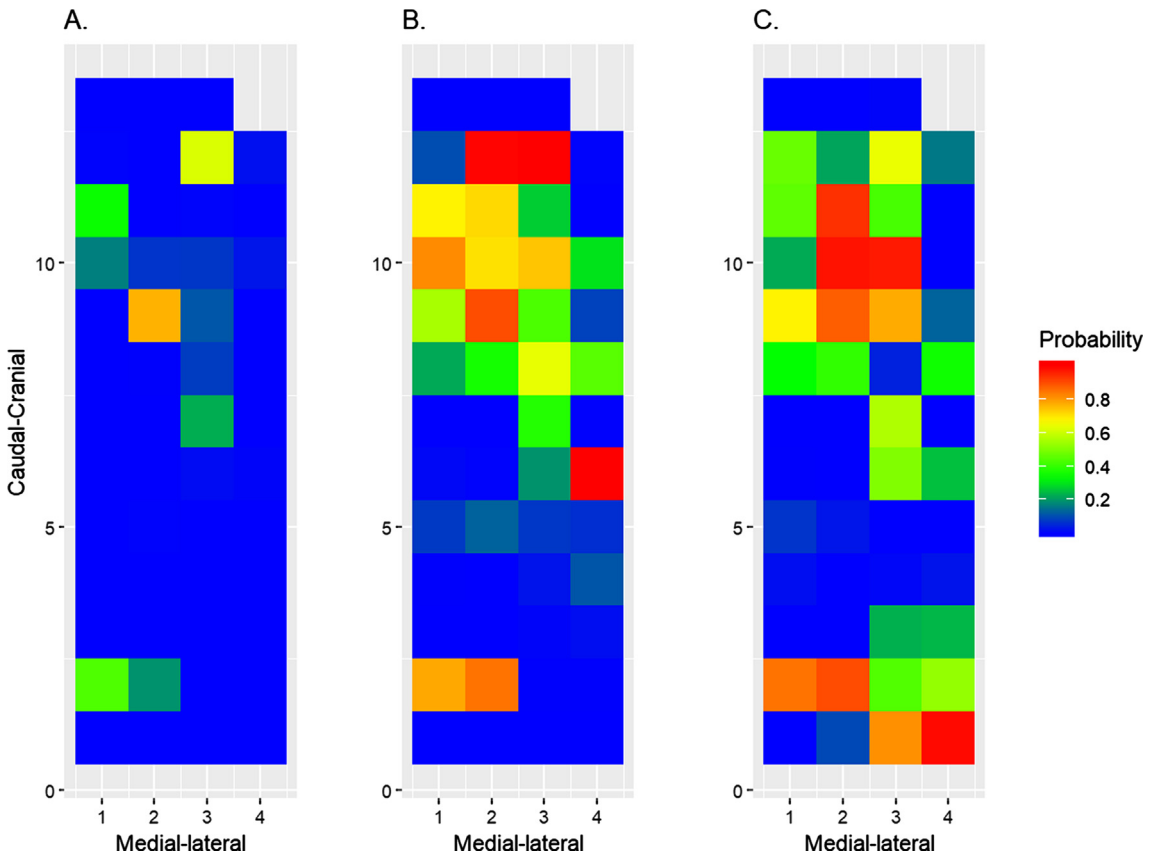

Fig 2. Joint probabilities of observing ΔEMG_{RMS} (independent of the lifting epochs) across any channels within the electrode grid between hypertonic saline injection and (A) baseline, (B) isotonic saline injection, and (C) recovery. Map colours represent joint probability values varying from 0 to 1.

3. Results

3.1. Comparing pairwise injection conditions during early lift phase

3.1.1. Main and interaction effects

There were significant spatial main and spatial-temporal interaction effects in EMG changes. To clarify, a spatial main effect is the influence of different EMG channel locations on EMG values (independent of lifting cycle); temporal main effect is the influence of different lifting cycles on EMG values (independent of channel location); and spatio-temporal interaction is the influence of different EMG channel locations at each lifting cycle on the EMG values. At the spatial main effect level, there was a > 0.95 probability that EMG changes were present between hypertonic saline injection and isotonic saline injection, and recovery conditions largely in the cranial half of the electrode grid (Fig. 2). At the interaction level, the period with the greatest number of spatial locations with > 0.95 probability of EMG changes was at 30% lift cycle between hypertonic injection-baseline conditions, 30% lift cycle between hypertonic-isotonic saline injections, and 30% between hypertonic injection-recovery conditions (Fig. 3).

3.1.2. Effect size of EMG RMS change (μV)

The maximal decrease in EMG RMS within the electrode grid after hypertonic saline injection was −38.1 μV [95% CrI −40.9 to −35.3] at 30% lift cycle when compared to baseline (Fig. 4). The maximal decrease in EMG RMS within the electrode grid after hypertonic saline injection was −28.8 μV [95% CrI −31.4 to −26.2] at 30% lift cycle when compared to recovery (Fig. 4). The maximal increase in EMG RMS within the electrode grid after hypertonic saline injection was 6.7 μV [95% CrI 4.1 to −9.3] at 80% of the lift cycle and this was compared to the recovery condition (Fig. 4).

3.2. Influence of lift phase on the effects of hypertonic injection

3.2.1. Main and interaction effects

There were significant spatial main and spatial-temporal interaction effects in EMG changes between lifting phases. At the spatial main effect level, there was a > 0.95 probability that the effects of hypertonic saline injection changed between the early and later lifting phases, independent of lifting cycle (Fig. 5). At the interaction level, the period with the greatest number of spatial locations with > 0.95 probability of EMG changes happening between lifting phases was at 80% lift cycle between hypertonic injection-baseline conditions, 80% lift cycle between hypertonic-isotonic saline injections, and 40% lift cycle between hypertonic injection-recovery conditions (Fig. 6).

3.2.2. Effect size of EMG RMS change (μV)

The reduction in EMG activity with hypertonic saline injection was predominantly greater during the early than in the later lifting phase, although there were some spatial locations where the reduction was less in the early than later lifting phase (Fig. 7). The maximal difference in EMG RMS reduction within the electrode grid during the early phase after hypertonic saline injection was 10.4 μV [95% CrI 8.2–12.6] more than the later phase at 80% lift cycle when compared to baseline; and by 5.8 μV [95% CrI 3.6–8.0] more than the later phase at 20% lift cycle when compared to recovery (Fig. 7).

4. Discussion

The main aim of the present study was to quantify the spatial distribution of upper trapezius activity under nociception that accounts for the reported shifts in its barycentre of activity. The Bayesian spatio-temporal ANOVA method used presently revealed three new findings which partially supported our hypotheses. First, an acute noxious

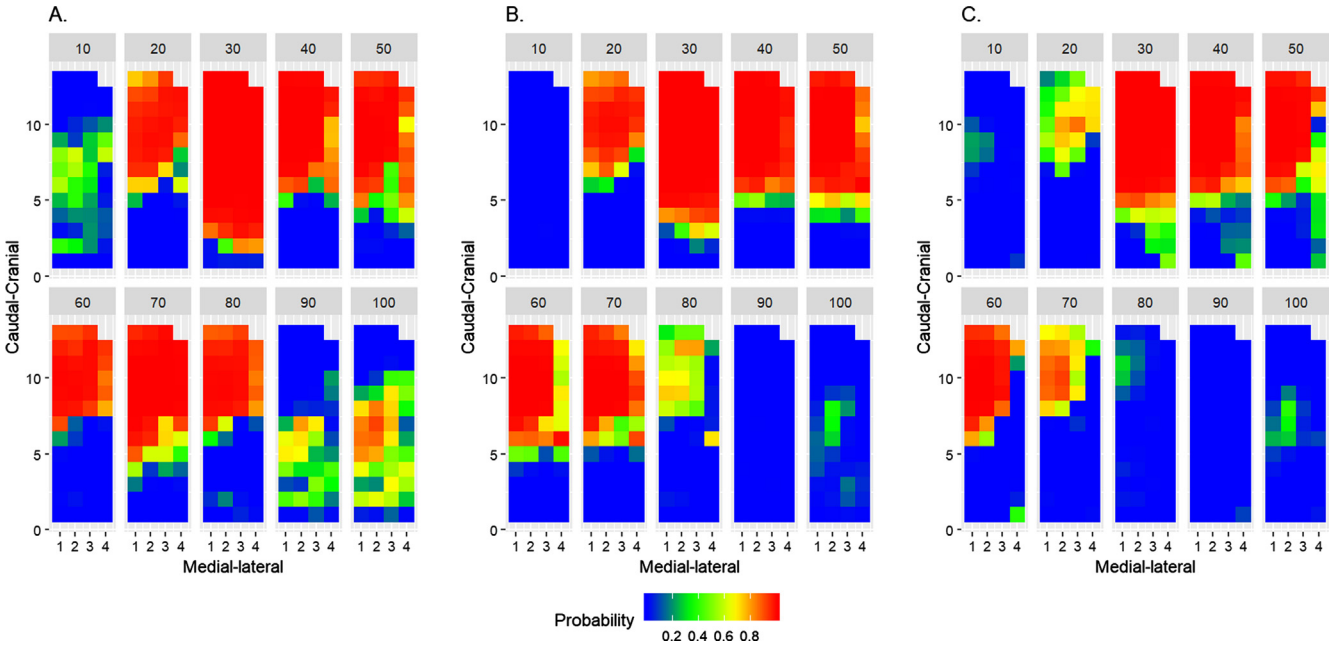

Fig 3. Joint probabilities of observing ΔEMG_{RMS} across any channels within the electrode grid between hypertonic saline injection and (A) baseline, (B) isotonic saline injection, and (C) recovery calculated at each 10% epoch. Map colours represent probability values varying from 0 to 1.

stimulus to the cranial upper trapezius reduced muscle activity within the same muscle region, and slightly increased activity in the caudal-most portion of the muscle. Second, there was a greater reduction of muscle activity detected on the medial compared to the lateral part of the recording surface during acute nociception. Third, differences in the effects of acute nociception between lifting phases predominantly lay in the cranial-caudal axis, rather than in the medial-lateral axis.

The present study provides evidence that the intra-muscular adaptation to acute nociception may be specific to the site of nociceptive stimulus (Gallina et al., 2018). Such an adaptation may be aimed at mechanically unloading the painful muscle region (Gallina et al., 2018). Location specific responses to acute nociception was observed in a previous study (Gallina et al., 2018), but not others (Dideriksen et al., 2016, Falla et al., 2009). Dideriksen et al. (2016) reported that the regional discharge rate of motor units of the upper trapezius was similar regardless of nociception site. Dideriksen et al. (2016) identified cranial motor units from the cranial six rows of the electrode grid, whilst caudal motor units were identified from the caudal six rows. The smaller the spatial separation of the motor units' sources, the more homogeneous will be their behaviour (Falla et al., 2017). However, the spatial correlation between extracted motor units were not considered during statistical inference, which may negatively influence the statistical model's validity (Dideriksen et al., 2016).

This is the first study to quantify the influence of acute nociception on the instantaneous spatial activity change of the upper trapezius. The periods of greatest reduction in amplitude of the cranial region of the

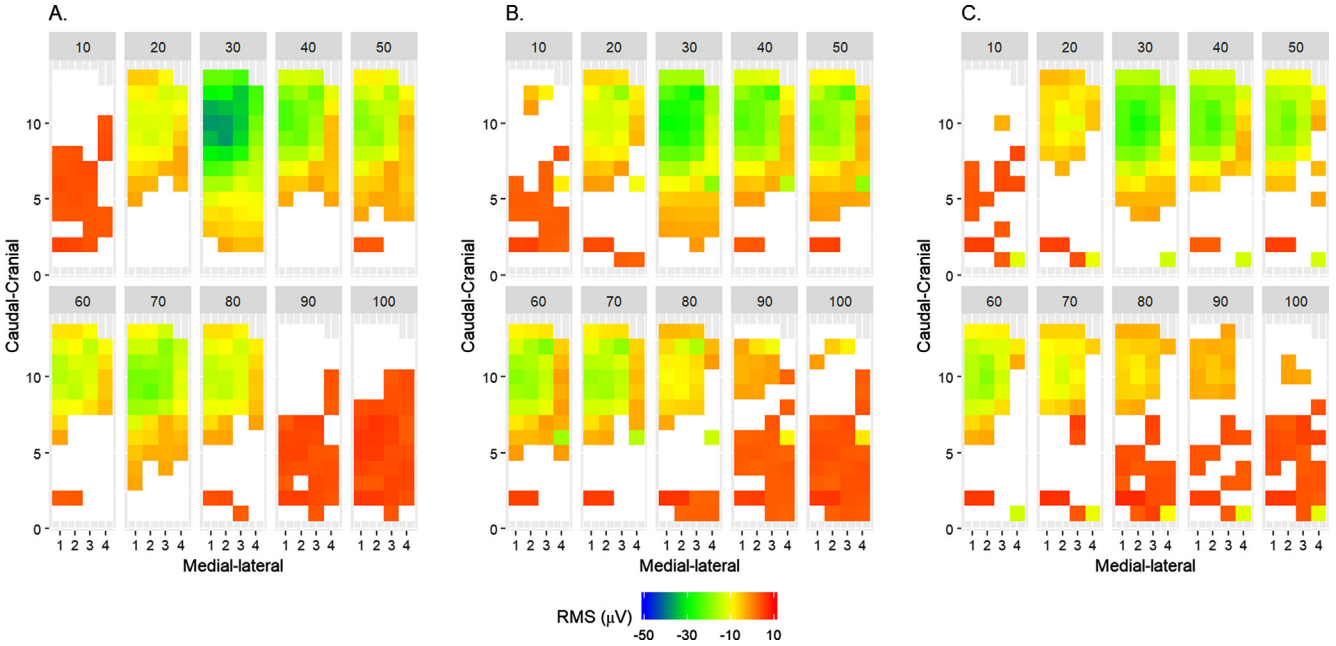

Fig 4. Effect sizes of significant ΔEMG_{RMS} (μV) induced by hypertonic saline injection, compared to (A) baseline, (B) isotonic saline injection, and (C) recovery calculated at each 10% epoch. Non-significant spatial regions where 95%CrI includes zero is coloured white.

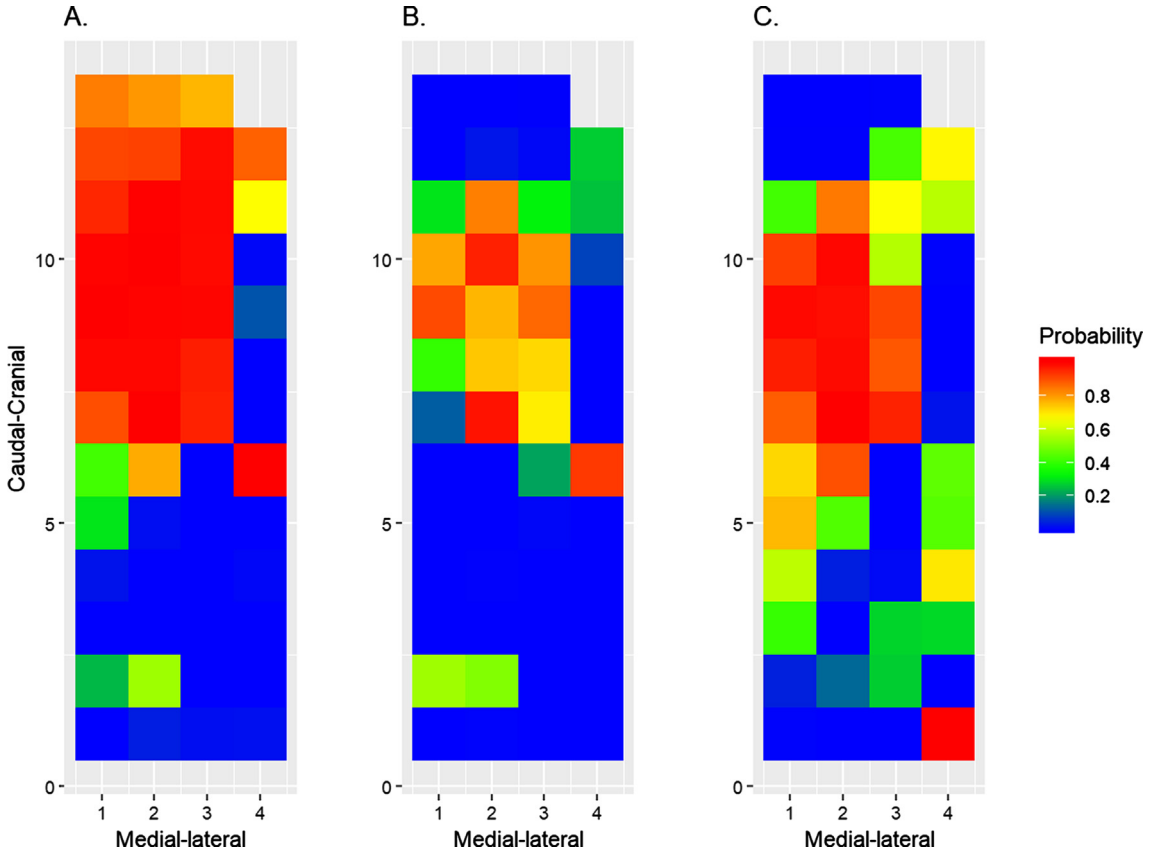

Fig 5. Joint probabilities of observing ΔEMG_{RMS} (independent of the lifting epochs) across any channels within the electrode grid between the early-later lifting phases in the effects of hypertonic saline injection compared to (A) baseline, (B) isotonic saline injection, and (C) recovery. Map colours represent probability values varying from 0 to 1.

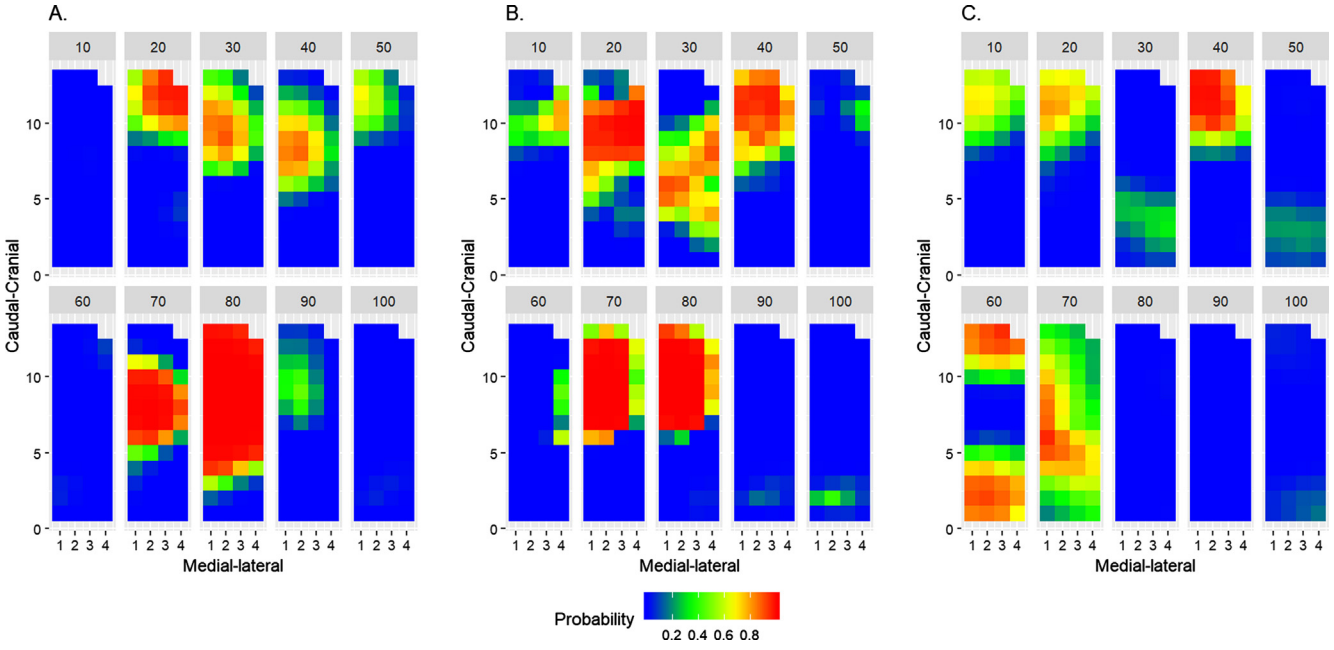

Fig 6. Joint probabilities of observing ΔEMG_{RMS} across any channels within the electrode grid between the early-later lifting phases in the effects of hypertonic saline injection compared to (A) baseline, (B) isotonic saline injection, and (C) recovery calculated at each 10% epoch. Map colours represent probability values varying from 0 to 1.

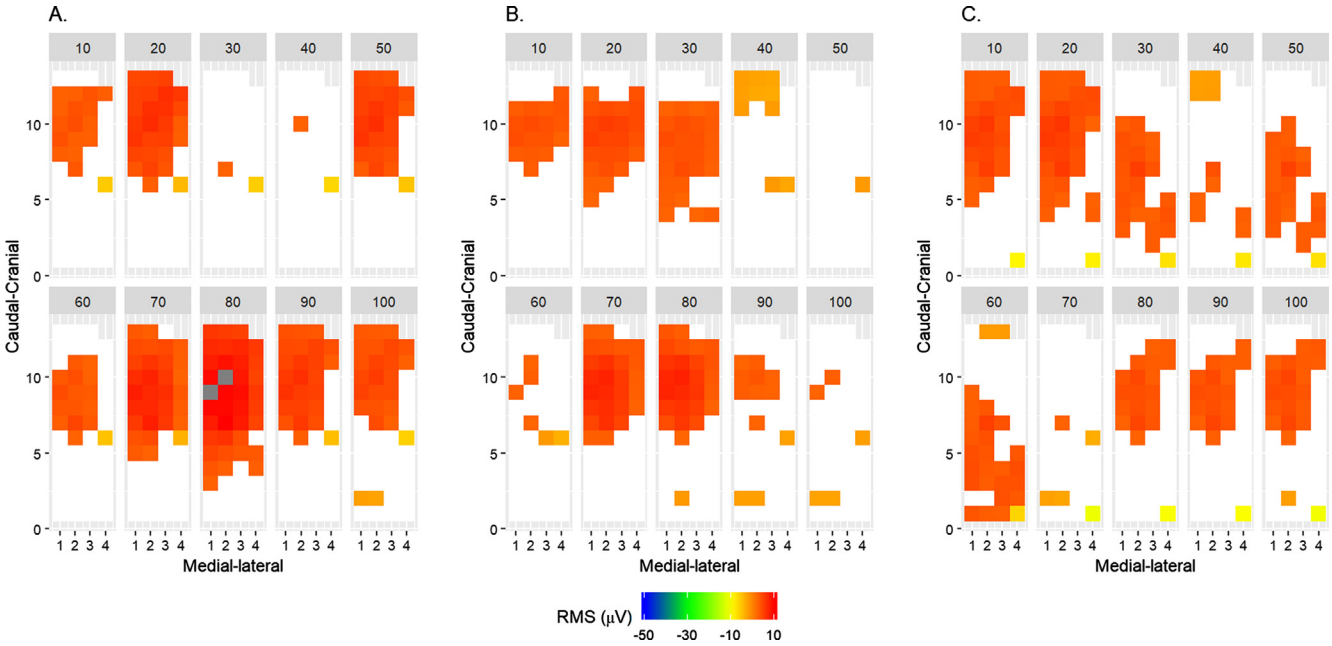

Fig 7. Effect sizes of significant ΔEMG_{RMS} (μV) between the early and later lifting phases induced by hypertonic saline injection, compared to (A) baseline, (B) isotonic saline injection, (C) recovery calculated at each 10% epoch. Non-significant spatial regions where 95%CrI includes zero is coloured white.

upper trapezius during acute nociception lay within periods when the cranial region was most active (20–70% of lifting cycle). This may be an optimal motor strategy to unload painful tissues as this represents a phase within the lifting cycle when mechanical load on the muscle would be greatest. The influence of acute nociception on a muscle's spatial distribution of activity appears to differ between dynamic and isometric contractions. Sustained isometric contraction results in greater activity within the cranial region of the upper trapezius (Madeleine et al., 2006, Falla et al., 2008). This increase in muscle activity may augment tissue loading to the cranial region of the muscle. To reduce pain associated with hypertonic saline injection, more activity should be reduced in the cranial region of the upper trapezius as the contraction duration increases to mechanically unload this region. This would mean observing a greater caudal shift in the upper trapezius barycentre as isometric contraction duration increases in the presence of nociception. Instead, previous studies observe that that caudal shift in the upper trapezius's barycentre remains constant regardless of isometric contraction duration (Madeleine et al., 2006, Falla et al., 2008).

The mechanisms explaining why nociception reduced muscle activity more when there was higher versus lower baseline amplitude is unclear. It may be that pain intensity was greatest between 20% and 70% of the lifting cycle, resulting in greater inhibition on the motorneuron pool (Farina et al., 2004). However, subjective pain recordings within a movement cycle in a repetitive dynamic task are difficult to collect. Alternatively, the inhibition to the recruited motorneurons of the upper trapezius may remain invariant, but the central excitability to the motorneurons may depend on the shoulder elevation angle. The relationship between central excitability of a muscle and shoulder elevation angles, has been shown for the infraspinatus (Lin et al., 2015), but not for the upper trapezius.

The medial-lateral coordinate of the upper trapezius's barycentre was reported to remain invariant with acute nociception (Falla et al., 2017, Madeleine et al., 2006, Dideriksen et al., 2016). The barycentre approach decomposes the shift in the centroid of muscle activity along two Cardinal axes within the plane of the electrode grid. The present study observed greater medial than lateral reductions of the EMG amplitude in the cranial two thirds of the upper trapezius with acute nociception. This means that the shift in the centroid of muscle activity under nociception would be caudal-laterally rather than purely within the longitudinal axis of the grid.

The reductive effect of acute nociception on muscle activity was greater in the early, than later lifting phases, which was most apparent in the cranial upper trapezius. Based on the mechanical unloading hypothesis (Gallina et al., 2018), additional muscle activity to sustain lifting ought to be recruited from the caudal upper trapezius, which has no noxious stimulus induced. It appears that compensatory motor adaptations associated with repetitive task performance and pain are competing in dynamic motor tasks. Speculatively, the caudal upper trapezius may receive more inhibitory afferent input, due to the accumulation of local extracellular potassium ions associated with prolonged contractions (Falla and Farina, 2008b). In addition, pain was decreasing from its maximum intensity in the later lifting phase (Falla et al., 2017). Given the greater nociceptive afferent distribution to the cranial than caudal region (Dideriksen et al., 2016), the reduction in pain intensity may preferentially reduce the inhibitory afferent input to the former compared to the latter region of the upper trapezius. It is unknown if compensatory neuromuscular adaptations associated with repetitive task performance (including fatigue) and pain are competing in dynamic motor tasks in clinical pain conditions.

This current work has several limitations. First, it was previously reported that acute nociception resulted in a similar caudal shift of the barycentre of upper trapezius activity between genders (Falla et al., 2008). Instead, the difference between genders lie in the interaction between nociceptive stimulation and fatigue, on the neuromuscular adaption of the upper trapezius (Falla et al., 2008). Given that only male participants were presently investigated, the influence of task repetition on the intramuscular adaptations observed with acute nociception should be generalized to female participants with caution.

Second, an injection was performed at a single location only in the present study. This limits the ability to conclude if intramuscular adaptations to nociception are dependent on the site of noxious stimulation within the upper trapezius. Nevertheless, the present study provides a specific intramuscular "signature" of how the upper trapezius activity shifts caudally relative to a specific site of nociception. Such knowledge, and indeed the proposed statistical method, is essential for future study designs where multiple sites of injection are used to investigate a muscle's response to the site of nociceptive activity.

Third, changes in EMG amplitudes during dynamic contractions

could be attributed to alterations in muscle geometry (Farina et al., 2001). The influence of altered muscle geometry on EMG activation cannot be eliminated but may be mitigated by averaging the EMG signals across lifting cycles (Farina et al., 2001). By including subject-level random effects into our statistical models, we simultaneously performed two procedures: (1) estimating a weighted average effect of acute nociception on EMG alterations per participant, and (2) using each participant's weighted average effect to estimate the overall group-level effect of acute nociception on the muscle's activity.

5. Conclusions

Motor adaptations to acute nociception appears to be region-specific in the upper trapezius, with a greater medial than lateral reduction in muscle activity. There also appears to be competing motor adaptations induced by nociception and repetitive task performance. Hence, mechanical unloading of painful tissues does not solely drive the motor adaptions observed with acute nociception during low-load lifting. The methods used in the present study provides a robust statistical inference method for spatio-temporal data, allowing a richer mechanistic insight into the motor adaptions that occur in response to pain

Declaration of Competing Interest

The authors declare no conflicts of interest and no financial disclosure.

Acknowledgements

None.

Appendix A. Supplementary material

Supplementary data to this article can be found online at https://doi.org/10.1016/j.jelekin.2019.05.018.

References

Abboud, J., Nougarou, F., Lardon, A., Dugas, C., Descarreaux, M., 2016. Influence of lumbar muscle fatigue on trunk adaptations during sudden external perturbations. Front. Hum. Neurosci. 10, 576. https://doi.org/10.3389/fnhum.2016.00576.

Bolin, D., Lindgren, F., 2015. Excursion and contour uncertainty regions for latent Gaussian models. J. R. Stat. Soc. Ser. B Stat. Methodol. 77, 85–106. https://doi.org/10.1111/rssb.12055.

Cameletti, M., Lindgren, F., Simpson, D., Rue, H., 2013. Spatio-temporal modeling of particulate matter concentration through the SPDE approach. Adv. Stat. Anal. 97, 109–131. https://doi.org/10.1007/s10182-012-0196-3.

Dideriksen, J.L., Holobar, A., Falla, D., 2016. Preferential distribution of nociceptive input to motoneurons with muscle units in the cranial portion of the upper trapezius muscle. J. Neurophysiol. 116, 611–618. https://doi.org/10.1152/jn.01117.2015.

Falla, D., Arendt-Nielsen, L., Farina, D., 2008. Gender-specific adaptations of upper trapezius muscle activity to acute nociceptive stimulation. Pain 138, 217–225. https://doi.org/10.1016/j.pain.2008.04.004.

Falla, D., Arendt-Nielsen, L., Farina, D., 2009. The pain-induced change in relative activation of upper trapezius muscle regions is independent of the site of noxious stimulation. Clin. Neurophysiol. 120, 150–157. https://doi.org/10.1016/j.clinph.2008.10.148.

Falla, D., Cescon, C., Lindstroem, R., Barbero, M., 2017. Muscle pain induces a shift of the spatial distribution of upper trapezius muscle activity during a repetitive task: a mechanism for perpetuation of pain with repetitive activity? Clin. J. Pain. 33, 1006–1013. https://doi.org/10.1097/ajp.0000000000000513.

Falla, D., Farina, D., 2008a. Motor units in cranial and caudal regions of the upper trapezius muscle have different discharge rates during brief static contractions. Acta Physiol. (Oxf.) 192, 551–558. https://doi.org/10.1111/j.1748-1716.2007.01776.x.

Falla, D., Farina, D., 2008b. Non-uniform adaptation of motor unit discharge rates during sustained static contraction of the upper trapezius muscle. Exp. Brain Res. 191, 363–370. https://doi.org/10.1007/s00221-008-1530-6.

Farina, D., Arendt-Nielsen, L., Merletti, R., Graven-Nielsen, T., 2004. Effect of experimental muscle pain on motor unit firing rate and conduction velocity. J. Neurophysiol. 91, 1250–1259. https://doi.org/10.1152/jn.00620.2003.

Farina, D., Merletti, R., Nazzaro, M., Caruso, I., 2001. Effect of joint angle on EMG variables in leg and thigh muscles. IEEE Eng. Med. Biol. Mag. 20, 62–71.

Gallina, A., Salomoni, S.E., Hall, L.M., Tucker, K., Garland, S.J., Hodges, P.W., 2018. Location-specific responses to nociceptive input support the purposeful nature of motor adaptation to pain. Pain 159, 2192–2200. https://doi.org/10.1097/j.pain.0000000000001317.

Hug, F., Hodges, P.W., Tucker, K.J., 2013. Effect of pain location on spatial reorganisation of muscle activity. J. Electromyogr. Kinesiol. 23, 1413–1420. https://doi.org/10.1016/j.jelekin.2013.08.014.

Liew, B., Yu, Y., Cescon, C., Barbero, M., Falla, D., 2018. HDsEMG data analysis using R-INLA. Mendeley Data v1. https://doi.org/10.17632/8hdb83vdvt.1.

Lin, Y.L., Christie, A., Karduna, A., 2015. Excitability of the infraspinatus, but not the middle deltoid, is affected by shoulder elevation angle. Exp. Brain Res. 233, 1837–1843. https://doi.org/10.1007/s00221-015-4255-3.

Madeleine, P., Leclerc, F., Arendt-Nielsen, L., Ravier, P., Farina, D., 2006. Experimental muscle pain changes the spatial distribution of upper trapezius muscle activity during sustained contraction. Clin. Neurophysiol. 117, 2436–2445. https://doi.org/10.1016/j.clinph.2006.06.753.

Martinez Valdes, E., Negro, F., Falla, D., De Nunzio, A.M., Farina, D., 2018. Surface EMG amplitude does not identify differences in neural drive to synergistic muscles. J. Appl. Physiol. https://doi.org/10.1152/japplphysiol.01115.2017.

Rue, H., Martino, S., Chopin, N., 2009. Approximate Bayesian inference for latent Gaussian models by using integrated nested Laplace approximations. J. R. Stat. Soc. Ser. B Stat. Methodol. 71, 319–392. https://doi.org/10.1111/j.1467-9868.2008.00700.x.

Samani, A., Srinivasan, D., Mathiassen, S.E., Madeleine, P., 2017. Variability in spatio-temporal pattern of trapezius activity and coordination of hand-arm muscles during a sustained repetitive dynamic task. Exp. Brain Res. 235, 389–400. https://doi.org/10.1007/s00221-016-4798-y.

Wang, X., Yu, Y., Faraway, J., 2018. Bayesian Regression Modeling with INLA. Chapman and Hall/CRC, Boca Raton, FL.

Yu, Y., Bolin, D., Rue, H., Wang, X., 2018. Bayesian generalized two-way ANOVA modeling for functional data using INLA. Stat. Sin. https://doi.org/10.5705/ss.202016.0055.

Dr. Bernard Liew is a Physiotherapist with a PhD in biomechanics. He currently works as a research fellow at the Centre of Precision Rehabilitation for Spinal Pain (CPR Spine), School of Sport, Exercise and Rehabilitation Sciences, College of Life and Environmental Sciences, University of Birmingham, Birmingham, United Kingdom.

Dr. Yu (Ryan) Yue has a PhD in statistics. He is currently an Associate Professor in Statistics at the Paul H. Chook Department of Information Systems and Statistics, Zicklin School of Business, Baruch College, CUNY, New York, United States.

Dr. Corrado Cescon has a PhD in Biomedical Engineering. He is currently a senior researcher and lecturer in the Department of Business Economics, Health and Social Care, University of Applied Sciences and Arts of Southern Switzerland, Manno, Switzerland.

Dr. Marco Barbero is a Physiotherapist with a PhD on the topic of myofascial trigger points. He is currently Associate Professor and Head of the Rehabilitation Research Laboratory (2rLab), in the Department of Business Economics, Health and Social Care, University of Applied Sciences and Arts of Southern Switzerland, Manno, Switzerland.

Dr Deborah Falla is a Physiotherapist with a PhD. She is currently a Professor and Chair in Rehabilitation Science and Physiotherapy at the University of Birmingham, UK; as well as the Director of the Centre of Precision Rehabilitation for Spinal Pain (CPR Spine).